Inorg. Chem. **2006**, *45*, 7777–7787

2-Aminopyrrolines: New Chiral Amidinate Ligands with a Rigid Well-Defined Molecular Structure and Their Coordination to Ti^{IV}

Benjamin D. Ward,[§] Hélène Risler,[#] Katharina Weitershaus,[§] Stéphane Bellemin-Laponnaz,*[,#] Hubert Wadepohl,[§] and Lutz H. Gade*[,§]

Anorganisch-Chemisches Institut, Universität Heidelberg, Im Neuenheimer Feld 270, 69120 Heidelberg, Germany, and Laboratoire de Chimie Organométallique et de Catalyse, Institut le Bel, Université Louis Pasteur, 4 rue Blaise Pascal, 67070 Strasbourg, France

Received May 11, 2006

The use of an amino-oxazolinate (NN_{ox} = κ^2-2,6-dimethylphenylamido-4(*S*)-isopropyloxazoline) as a chiral analogue to amidinate ligands in the chemistry of titanium was found to lead to undesired side reactions. The reaction of 2,6-dimethylphenylamido-4(*S*)-isopropyloxazoline with $[Ti(NMe_2)_4]$ afforded the bis(amidinato) complex $[Ti(NN_{ox})_2(NMe_2)_2]$ (**2**) which was thermally converted to the ring-opened decomposition products $[Ti(NN_{ox})\{\kappa^3\text{-}N(2,6\text{-}C_6H_3Me_2)C(NMe_2)NC(^iPr)CH_2O\}(NMe_2)]$ (**3**) and $[Ti\{\kappa^3\text{-}N(2,6\text{-}C_6H_3Me_2)C(NMe_2)\text{-}NC(^iPr)CH_2O\}_2]$ (**4**). The NMR spectra of **4** recorded at low temperature displayed two sets of resonances corresponding to two symmetric isomers in a 2:5 ratio, the probable geometries of which were established by ONIOM (QM/MM) simulations. To suppress ring opening of the oxazolines, their oxygen atom was formally replaced by a CH_2 group in the synthesis of a series of amino-pyrroline protioligands 2-RN(H)(5-C_4H_5NR') ($HN^RN^{R'}$). Their reaction with $[Ti(NMe_2)_4]$ gave the thermally stable complexes $[Ti(N^RN^{R'})_2(NMe_2)_2]$, of which three derivatives were characterized by X-ray diffraction. They are stereochemically dynamic and undergo reversible ligand rearrangements in solution, for which the activation parameters were determined by variable-temperature ^1H NMR spectroscopy.

Introduction

The reactivity of a metal complex is controlled, to a large extent, by the choice of the spectator (or "ancillary") ligands. These not only determine the electronic structure of the metal center but also generate the shape of the active space of the coordination sphere at which the chemical transformations take place. An efficient design of such ancillary ligands is based on a well-defined molecular structure with reduced conformational degrees of freedom. Frequently, the possibility of variable denticity of the spectator ligands, allowing the system to "open up" during the course of a metal-centered reaction, is exploited to enhance their chemical reactivity in stoichiometric and catalytic transformations.[1]

Metal-coordinated amidinates have been proven to provide a versatile supporting ligand environment in organometallic and coordination chemistry.[2,3] Ever since the pioneering work by Brunner,[4] Roesky,[5] Dehnicke,[6,7] and Edelmann,[8−10] there have been few metals to which amidinate ligands have not been coordinated. In recent years, amidinates have been shown to be ideal ancillary ligands for a variety of early transition metals, including group 3 and lanthanides,[11−14] as

* To whom correspondence should be addressed. Phone: +49-6221-548443 (L.H.G.); +33-390-241542 (S.B.-L.). E-mail: lutz.gade@uni-hd.de (L.H.G.); bellemin@chimie.u-strasbg.fr (S.B.-L.).
[§] Universität Heidelberg.
[#] Université Louis Pasteur.

(1) *Comprehensive Coordination Chemistry Vol. 1*; McCleverty, J.A., Meyer, T. J., Eds.; Elsevier Pergamon: Amsterdam, 2003; Sections I and III.
(2) Barker, J.; Kilner, M. *Coord. Chem. Rev.* **1994**, *133*, 219.
(3) Edelmann, F. T. *Coord. Chem. Rev.* **1994**, *137*, 403.
(4) Brunner, H.; Lukassek, J.; Agrifoglio, G. *J. Organomet. Chem.* **1980**, *195*, 63.
(5) Roesky, H. W.; Meller, B.; Noltemeyer, M.; Schmidt, H. G.; Scholz, U.; Sheldrick, G. M. *Chem. Ber.* **1988**, *121*, 1403.
(6) Fenske, D.; Hartmann, E.; Dehnicke, K. *Z. Naturforsch. B* **1988**, *43*, 1611.
(7) Dehnicke, K.; Ergezinger, C.; Hartmann, E.; Zinn, A.; Hoesler, K. *J. Organomet. Chem.* **1988**, *352*, C1.
(8) Wedler, M.; Knoesel, F.; Edelmann, F. T.; Behrens, U. *Chem. Ber.* **1992**, *125*, 1313.
(9) Wedler, M.; Recknagel, A.; Gilje, J. W.; Nottemeyer, M.; Edelmann, F. T. *J. Organomet. Chem.* **1992**, *426*, 295.
(10) Recknagel, A.; Knoesel, F.; Gornitzka, H.; Noltemeyer, M.; Edelmann, F. T.; Behrens, U. *J. Organomet. Chem.* **1991**, *417*, 363.
(11) Skinner, M. E. G.; Mountford, P. *J. Chem. Soc., Dalton Trans.* **2002**, 1694.
(12) Hagadorn, J. R.; Arnold, J. *Organometallics* **1996**, *15*, 984.
(13) Edelmann, F. T.; Richter, J. *Eur. J. Solid State Inorg. Chem.* **1996**, *33*, 157.

10.1021/ic060809y CCC: $33.50
Published on Web 08/22/2006

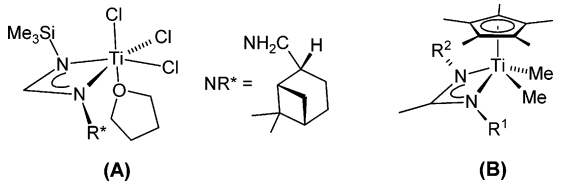

Figure 1. Amidinato ligands employed to generate chiral reaction sites, either by introducing chiral substituents at the N atoms (**A**) or by a nonsymmetrical substitution pattern at the amidinato function which induces metal centered chirality (**B**).

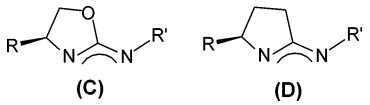

Figure 2. 2-Aminooxazoline (**C**) and 2-Aminopyrroline (**D**) based chiral amidinato ligands.

well as for metals from groups 4[15−21] and 5.[22,23] Amidinato ligands have also been employed to generate chiral reaction sites, either by introducing chiral substituents at the N atoms, as shown by Eisen and co-workers (**A** in Figure 1)[27] or by a nonsymmetrical substitution pattern at the amidinato function (**B** in Figure 1). Upon coordination to an appropriate metal complex fragment the latter induces metal-centered chirality, a concept which has been actively investigated in Sita's group (Figure 1b). Both Sita and Eisen have reported group 4 complexes derived from these amidinates, which have been proven to be remarkably efficient for the stereoselective polymerization of α-olefins.[24−28]

A further advance into the chemistry of chiral amidinates has been made by Scott, who has reported the synthesis of amino-oxazoline ligands, which are effectively chiral amidinate analogues (**C** in Figure 2).[29] In these ligands, the chirality is effected by including one of the amidinate nitrogen atoms and the central bridging carbon atom in a rigid cyclic structure which contains a stereocenter, in this case an oxazoline ring. Such a ligand architecture is ideal for the study of asymmetric catalysis with amidinate-supported metal complexes and forms a void in the chemical literature which warrants further investigation.

Scheme 1. Synthesis of the 2-Amidooxazoline Derivative, **1**, Using the Strategy Developed by Lee and Scott and Coordination of the Oxazoline-Based Amidinate to Titanium(IV)

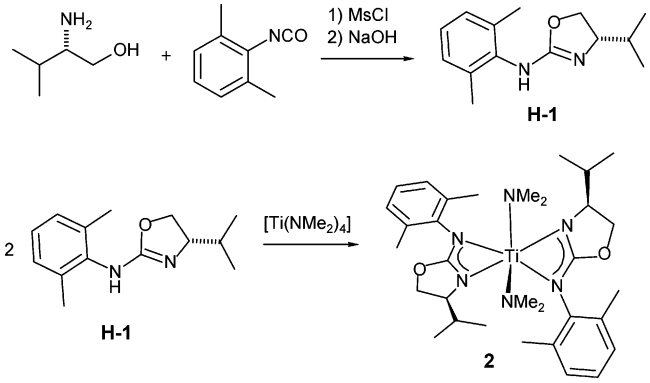

As part of our continued investigation into new chiral ligands in coordination chemistry and catalysis, we have investigated the synthesis and reactivity of titanium amino-oxazoline complexes. However, as will be reported in this work, we have found that, although the titanium amide complex $[Ti(NN_{ox})_2(NMe_2)_2]$ (NN_{ox} = κ^2-2,6-dimethylphenylamido-4(*S*)-isopropyloxazoline) can be easily prepared, it proved to be unstable with respect to ligand degradation via C═N insertion into the amido−metal bonds. This has led us to redesign the ligand system by preparing the more robust amino-pyrroline derivatives (**D** in Figure 2) in which the oxygen is replaced by a methylene group, thus preventing the ring-opening decomposition pathway.

Results and Discussion

Synthesis of a Titanium Complex with Two Aminooxazolinato Ligands and its Thermal Degradation via C═N Insertion into the Metal−Amido Bonds and Ring Opening. The amino-oxazoline ligand HNN_{ox}, **H-1**, was synthesized according to a procedure inspired by Lee et al. and subsequently employed by Scott,[29] using (*S*)-valinol and 2,6-dimethylphenyl isocyanate (Scheme 1).[30] The subsequent reaction of the protioligand with $Ti(NMe_2)_4$ afforded the bis-(amidinato) complex $[Ti(NN_{ox})_2(NMe_2)_2]$ (**2**). Complex **2** was formed regardless of the stoichiometry used in the reaction and consequently the complex containing only a single amidinate ligand could not be obtained.

The NMR spectra of **2** are consistent with a highly symmetrical species, whereas when the spectra are recorded at low temperature, the signals broaden and decoalesce, indicating the presence of two isomeric forms. These observations are consistent with an overall rotation of the amidinate ligands, which is rapid at room temperature. Although the low-temperature spectra clearly suggest that there are two species present, the fluxional process could not be completely "frozen out" within the instrumental

(14) Bambirra, S.; Bouwkamp, M. W.; Meetsma, A.; Hessen, B. *J. Am. Chem. Soc.* **2004**, *126*, 9182.
(15) Li, C.; Thomson, R. K.; Gillon, B.; Patrick, B. O.; Schafer, L. L. *Chem. Commun.* **2003**, 2462.
(16) Littke, A.; Sleiman, N.; Bensimon, C.; Richeson, D. S.; Yap, G. P. A.; Brown, S. J. *Organometallics* **1998**, *17*, 446.
(17) Keaton, R. J.; Jayaratne, K. C.; Henningsen, D. A.; Koterwas, L. A.; Sita, L. R. *J. Am. Chem. Soc.* **2001**, *123*, 6197.
(18) Kissounko, D. A.; Zhang, Y.; Harney, M. B.; Sita, L. R. *Adv. Synth. Catal.* **2004**, *347*, 426.
(19) Guiducci, A. E.; Boyd, C. L.; Mountford, P. *Organometallics* **2006**, *25*, 1167.
(20) Boyd, C. L.; Clot, E.; Guiducci, A. E.; Mountford, P. *Organometallics* **2005**, *24*, 2347.
(21) Guiducci, A. E.; Cowley, A. R.; Skinner, M. E. G.; Mountford, P. *J. Chem. Soc., Dalton Trans.* **2001**, 1392.
(22) Brussee, E. A. C.; Meetsma, A.; Hessen, B.; Teuben, J. H. *Chem. Commun.* **2000**, 497.
(23) Pugh, S. M.; Trösch, D. J. M.; Skinner, M. E. G.; Gade, L. H.; Mountford, P. *Organometallics* **2001**, *20*, 3531.
(24) Zhang, Y.; Reeder, E. K.; Keaton, R. J.; Sita, L. R. *Organometallics* **2004**, *23*, 3512.
(25) Zhang, Y.; Sita, L. R. *Chem. Commun.* **2003**, 2358.
(26) Jayaratne, K. C.; Sita, L. R. *J. Am. Chem. Soc.* **2000**, *122*, 958.
(27) Averbuj, C.; Tish, E.; Eisen, M. R. *J. Am. Chem. Soc.* **1998**, *120*, 8640.
(28) Volkis, V.; Shmulinson, M.; Averbuj, C.; Lisovskii, A.; Edelmann, F. T.; Eisen, M. R. *Organometallics* **1998**, *17*, 3155.
(29) (a) Munslow, I. J.; Wade, A. R.; Deeth, R. J.; Scott, P. *Chem. Commun.* **2004**, 2596. (b) Westmoreland, I.; Munslow, I. J.; Clarke, A. J.; Clarkson, G.; Scott, P. *Organometallics* **2004**, *23*, 5066.
(30) Kim, T. H.; Lee, N.; Lee, G.; Kim, J. N. *Tetrahedron* **2001**, *57*, 7137.

Scheme 2. Thermally Induced Migration of the NMe_2 Ligands and the Concommitant Opening of the Oxazoline Rings of the Bis(2-amido-oxazoline)titanium Complex **2** via **3** to Give the $Ti(NNO)_2$ Complex **4**

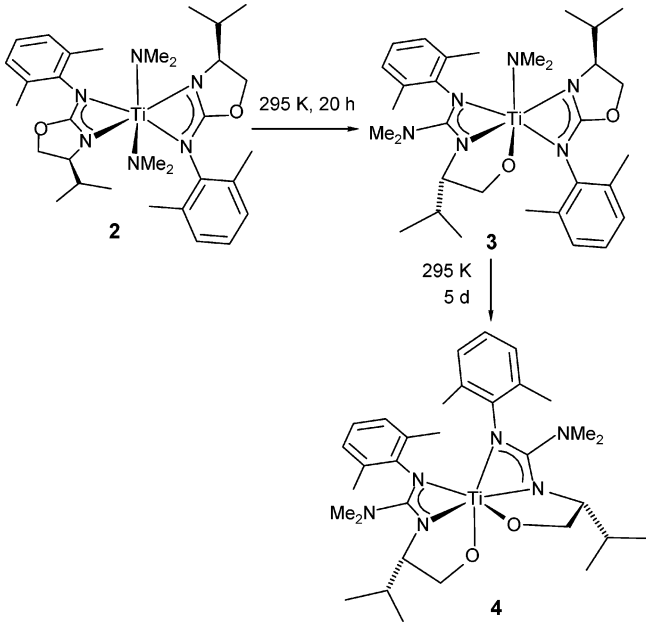

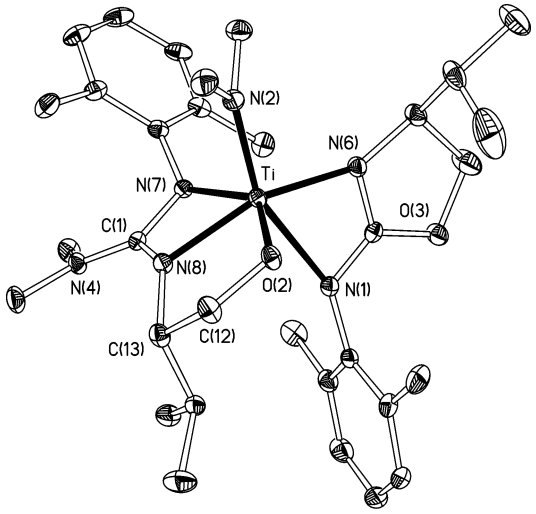

Figure 3. Molecular Structure of **3**. Thermal ellipsoids are drawn at 25% probability, and the H atoms have been omitted for clarity. Principal bond lengths (Å) and angles (deg): Ti−N(2) = 1.898(3), Ti−N(1) = 2.444(3), Ti−N(6) = 2.079(3), Ti−N(7) = 2.149(3), Ti−N(8) = 2.028(3), Ti−O(2) = 1.853(3), N(1)−Ti−N(2) = 156.99(12), N(6)−Ti−N(1) = 59.44(11), N(7)−Ti−N(8) = 62.59(12), N(2)−Ti−N(6) = 97.57(13), N(2)−Ti−O(2) = 98.21(13), N(2)−Ti−N(7) = 96.59(14), N(2)−Ti−N(8) = 107.71(14).

capability in our laboratories (400 MHz, −80 °C); however, we have been able to successfully determine the nature of this fluxional process with the related amino-pyrroline-based complexes (vide infra) and further discussion will be provided in the following section.

Complex **2**, although isolated and characterized, was found to be unstable, and samples of **2** at ambient temperature readily undergo a rearrangement by migration of the metal-bonded amide ligands to the C═N bonds of the oxazoline groups. This leads to ring-opening of the oxazolines and, consequently, to products containing either one or two κ^3-bound mixed amidinate-alkoxide ligands (Scheme 2). Ring-opening decomposition pathways are well-known in oxazoline chemistry but are mostly induced by Lewis or Brønsted acids.[31] A sample of **2** was monitored by NMR spectroscopy over a one week period to follow the decomposition process.

The onset of decomposition occurs within 1 h at ambient temperature. After standing for 20 h, the spectra contained signals corresponding to two species in solution in addition to **2**, the major product being unsymmetrical. As indicated above, we attribute this set of signals to the product of a migration of an N-bonded dimethylamido ligand to the backbone of one of the oxazoline amidinates, amounting to the formal oxazoline C═N insertion into the metal−amido bond [$Ti(NN_{ox})\{\kappa^3$-$N(2,6\text{-}C_6H_3Me_2)C(NMe_2)$-$NC(^iPr)CH_2O\}$-$(NMe_2)$] (**3**). This leads to the conversion of one of the oxazolines to a dianionic tridentate N,N,O-ligand. The symmetrical resonance set (of the minor product) is attributed to the product of the equivalent transformation at the second oxazoline ring [$Ti\{\kappa^3$-$N(2,6\text{-}C_6H_3Me_2)C(NMe_2)NC(^iPr)$-$CH_2O\}_2$] (**4**). After ∼5 days, the second amide insertion reaction had gone to completion, with the NMR spectra showing the presence of **4** alone. The observation that this reaction product was formed along with a small amount of nonspecific degradation of the complexes in solution precluded a more detailed kinetic analysis of this process. When the partially converted reaction mixture containing all three complexes **2**, **3**, and **4** was cooled, X-ray quality crystals of **3** were formed. In addition, recrystallization of pure samples of **4**, isolated after complete consumption of its precursors, afforded X-ray quality crystals. These two structures have allowed us to confirm the nature of the decomposition pathway depicted in Scheme 2. The molecular structures of **3** and **4** are shown in Figures 3 and 4, respectively, along with the principal bond lengths and angles.

Complex **3** exhibits a highly distorted octahedral geometry about the titanium atom with the ring-opened (dianionic) alkoxy-amidinate ligand occupying a pseudomeridional coordination mode (Figure 3). The bond lengths of the coordinated atoms are unremarkable, with the exception of the amidinate nitrogen N(1), for which the Ti−N distance of 2.444(3) Å is somewhat larger than those previously reported (1.953−2.264, mean 2.101 Å for 65 examples),[32,33] presumably because of the trans influence of the strongly π-donating NMe_2 ligand. Similarly, the structure of **4** also exhibits a distorted octahedral geometry; however, in contrast to **3**, the alkoxy-amidinate ligands occupy pseudofacial coordination geometries, with each ligand moiety related to the other via a (noncrystallographic) C_2 rotation axis (Figure 4).

The ^{1}H NMR spectra of **4**, although highly symmetrical at ambient temperature, broaden and decoalesce upon cooling to −10 °C, affording signals corresponding to two symmetric isomers (i.e., with each species having signals for only a single ligand environment) in a 2:5 ratio. Although the NMR

(31) Kazi, A. B.; Jones, G. D.; Vicic, D. A. *Organometallics* **2005**, *24*, 6051.

(32) Allen, F. H.; Kennard, O. *Chem. Des. Autom. News* **1993**, *8*, 1 and 31.

(33) Fletcher, D. A.; McMeeking, R. F.; Parkin, D. *J. Chem. Inf. Comput. Sci.* **1996**, *36*, 746.

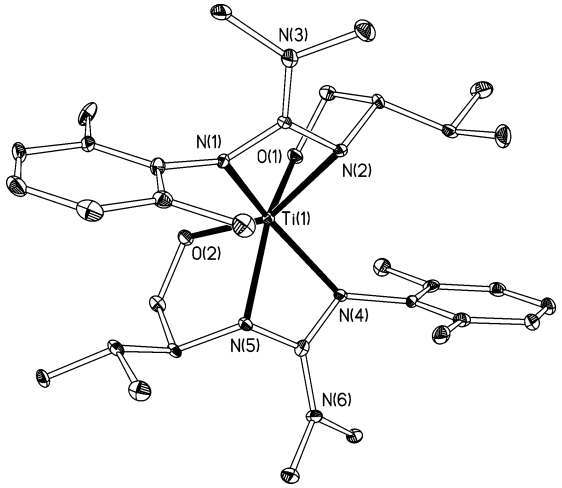

Figure 4. Molecular Structure of **4**. Thermal ellipsoids are drawn at 25% probability, and the H atoms have been omitted for clarity. Principal bond lengths (Å) and angles (deg): Ti(1)−N(1) = 2.094(3), Ti(1)−N(2) = 2.153(3), Ti(1)−N(4) = 2.094(3), Ti(1)−N(5) = 2.136(3), Ti(1)−O(1) = 1.865(2), Ti(1)−O(2) = 1.862(2), N(1)−Ti(1)−N(2) = 62.37(10), N(1)−Ti(1)−N(4) = 141.69(11), N(2)−Ti(1)−N(4) = 97.01(11), N(1)−Ti(1)−N(5) = 97.19(11), N(2)−Ti(1)−N(5) = 118.90(11), N(4)−Ti(1)−N(5) = 63.24(10), N(1)−Ti(1)−O(1) = 108.42(11), N(2)−Ti(1)−O(1) = 78.75(11), N(4)−Ti(1)−O(1) = 97.42(11), N(5)−Ti(1)−O(1) = 153.92(11), N(1)−Ti(1)−O(2) = 96.75(11), N(2)−Ti(1)−O(2) = 153.20(11), N(4)−Ti(1)−O(2) = 109.53(11), N(5)−Ti(1)−O(2) = 78.10(10), O(1)−Ti(1)−O(2) = 93.75(11).

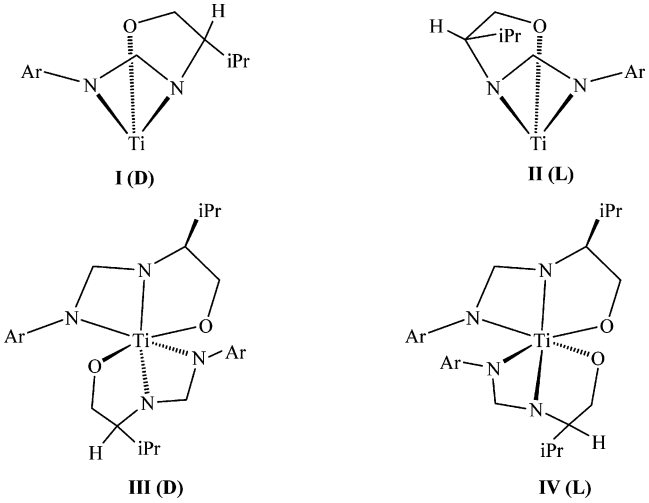

Figure 5. Possible coordination isomers of **4**. NMe_2 fragments and the second alkoxy-amidinate ligand **I** and **II** are omitted for clarity. Principal bond lengths (Å) and angles (deg): Ti(1)−N(1) = 2.094(3), Ti(1)−N(2) = 2.153(3), Ti(1)−N(4) = 2.094(3), Ti(1)−N(5) = 2.136(3), Ti(1)−O(1) = 1.865(2), Ti(1)−O(2) = 1.862(2), N(1)−Ti(1)−N(2) = 62.37(10), N(1)−Ti(1)−N(4) = 141.69(11), N(2)−Ti(1)−N(4) = 97.01(11), N(1)−Ti(1)−N(5) = 97.19(11), N(2)−Ti(1)−N(5) = 118.90(11), N(4)−Ti(1)−N(5) = 63.24(10), N(1)−Ti(1)−O(1) = 108.42(11), N(2)−Ti(1)−O(1) = 78.75(11), N(4)−Ti(1)−O(1) = 97.42(11), N(5)−Ti(1)−O(1) = 153.92(11), N(1)−Ti(1)−O(2) = 96.75(11), N(2)−Ti(1)−O(2) = 153.20(11), N(4)−Ti(1)−O(2) = 109.53(11), N(5)−Ti(1)−O(2) = 78.10(10), O(1)−Ti(1)−O(2) = 93.75(11).

data do not allow us to unambiguously determine the identity of the isomers, a consideration of the two X-ray structures indicates that there are two coordination modes (fac and mer) of the alkoxy-amidinate moiety, giving rise to four possible isomers which would each give C_2-symmetric NMR spectra (Figure 5). A fac coordination of the ligand would give rise to two possible isomers, D (**I**) and L (**II**). The two isomers

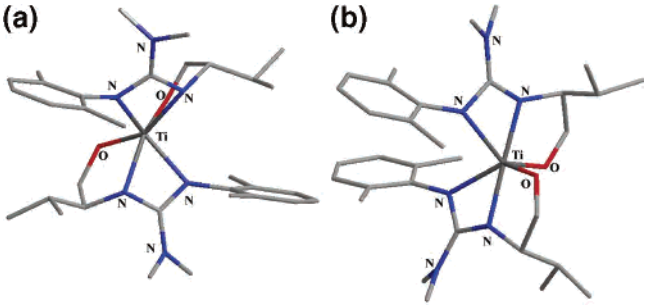

Figure 6. (a) ONIOM (B3PW91:UFF) calculated structure of **4**, isomer **I**. (b) ONIOM (B3PW91:UFF) calculated structure of **4**, isomer **III**.

differ in that the isopropyl group is directed exo (**I**) or endo (**II**) with respect to the N−N−O "pocket". Of the two possibilities, the D isomer (**I**) is that observed in the X-ray crystallographic study. A mer coordination of the ligand would also allow for two isomers D (**III**) and L (**IV**), in which the relative orientation of the N−N−O planes differ by 180°.

The four isomeric forms were calculated using the ONIOM (QM/MM) hybrid methodology. The metal and ligand backbone were modeled at the DFT level, with the isopropyl groups and aryl-methyl groups added at the molecular mechanics (UFF) level.

Of the four isomeric forms, only two gave a stable minimum after a geometry optimization: **I** and **III**. Structure **II** proved to be inherently unstable, and the calculation converged to **I**. This is presumably because of the unsatisfactory steric strain imposed by the endo isopropyl group. The calculation of **IV** successfully converged to a stable structure; however, an analysis of the frequency calculation indicated that the computed structure was in fact a saddle point and not a true minimum. No satisfactory minimum was obtained, regardless of the level of theory employed. The calculated structure of **I** gave a satisfactory minimum and is, moreover, representative of the X-ray structure for **4**, and thus, it provides a clarification that the calculations are reliable, as well as providing a useful comparison between experiment and theory. Upon comparing the molecular parameters between the calculated and X-ray structures, we found an excellent agreement between the two, with the differences in bond lengths being only marginally longer than the standard uncertainty in the X-ray measurement.

In contrast to the meridional isomer **IV**, calculations of **III** were successful and gave a stable minimum. The energy difference between the two successfully computed isomers was found to be only 3.0 kcal mol^{-1}, with **I** being the more stable of the two. Consideration of the entropic effects allowed us to compute the free energy values, although this had a negligible effect on the overall free enthalpy difference, being marginally reduced to 2.4 kcal mol^{-1}. We conclude from these studies that the experimentally observed isomers are likely to be those corresponding to isomers **I** and **III**, although it is inappropriate to comment on the energy difference further since this is likely to be within the error limits of the methodology employed. The calculated structures of **I** and **III** are provided in Figure 6a and b, respectively.

Scheme 3. General Synthesis of the 2-Aminopyrrolines **H-5**−**H-9**

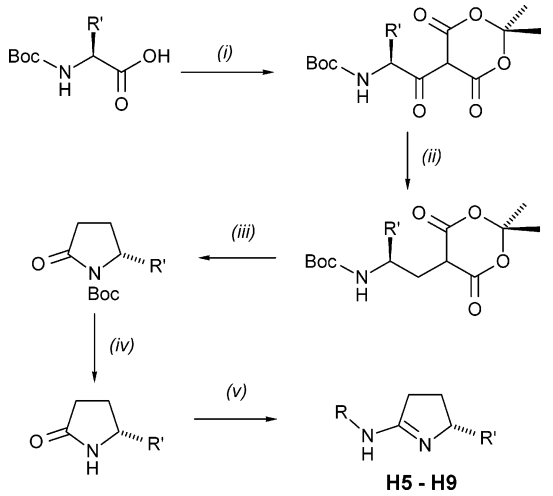

(i) 1.5 equiv of Meldrum's acid, 1.5 equiv of DMAP, 1.1 equiv of DCC, CH_2Cl_2; (ii) acetic acid, 2.6 equiv of $NaBH_4$, CH_2Cl_2; (iii) toluene, reflux; (iv) 5 equiv of $Mg(OMe)_2$, MeOH, or TFA/CH_2Cl_2; (v) first 3 equiv of pyridine and 1.2 equiv of Tf_2O, then 3 equiv of RNH_2.

Scheme 4. Synthesis of the Bis(2-amidopyrrolidin)titanium Complexes **10**−**14**

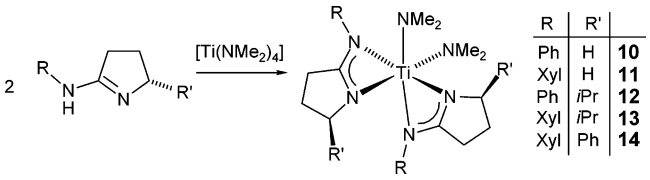

R	R′	
Ph	H	**10**
Xyl	H	**11**
Ph	*i*Pr	**12**
Xyl	*i*Pr	**13**
Xyl	Ph	**14**

Synthesis of 2-Aminopyrolidines. To avoid these ring-opening reactions, the oxygen atom in the oxaozoline ring of the chiral amidinato ligands was formally replaced by a CH_2 group. A series of these amino-pyrroline protioligands 2-RN(H)(5-C_4H_5NR′) (hereafter denoted $HN^RN^{R'}$) **H-5**−**H-8** was prepared, as illustrated in Scheme 3. The chiral amidines $HN^{Ph}N^{Pr}$ (**H-7**) and $HN^{Xyl}N^{Pr}$ (**H-8**) were obtained from the commercially available Boc-protected natural amino acid in 5 steps.

Boc-Val-OH was converted into the corresponding chiral pyrrolidinone in good overall yield after a sequence of four steps (55%, R′ = ^{i}Pr).[34] The final step involves the conversion of the lactam into the amidine derivative. Classical methods of conversion of the lactam into the imino ether with Meerwein's reagent, followed by reaction with arylamine gave essentially no product.[35] However, activation with trifluoromethanesulfonic (triflic) anhydride in the presence of pyridine according to Charette et al. gave a highly reactive intermediate which was treated in situ with arylamine.[36,37] With the use of this procedure, four amidines (R′ = H, ^{i}Pr) could be isolated in ∼25% overall yield as pale yellow oils.

To probe the limits of this synthetic strategy, we attempted to prepare the phenyl derivative (R′ = Ph). It is well-known that a phenyl group directly attached to a stereogenic carbon atom renders the system more prone to racemization. We were able to successfully prepare the xylyl-substituted amidine $HN^{Xyl}N^{Ph}$ (**H-9**) in ∼25% yield; however, the ligand could not be prepared without undergoing racemization. The racemization took place upon reduction of the coupling products of the protected amino acid with meldrums acid with $NaBH_4$ (step ii in Scheme 4) to move the carbonyl function in the α-position to the amino group. This indicates that there are limitations to the general procedure, and other than preparing a titanium complex to verify the structure of the ligand (vide infra), we have thus confined our studies to the alkyl, rather than aryl, derivatives.

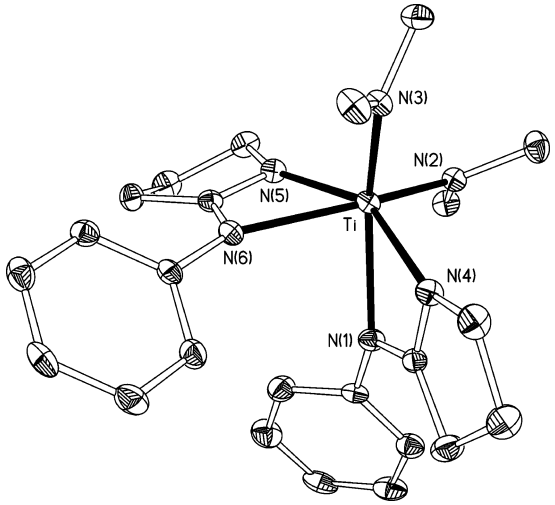

Figure 7. Molecular Structure of **10**. Thermal ellipsoids are drawn at 25% probability, and the H atoms have been omitted for clarity. Principal bond lengths (Å) and angles (deg): Ti−N(1) = 2.267(2), Ti−N(4) = 2.081(3), Ti−N(2) = 1.906(2), Ti−N(3) = 1.902(2), Ti−N(5) = 2.094(3), Ti−N(6) = 2.244(2), N(5)−Ti−N(6) = 61.56(9), N(1)−Ti−N(4) = 61.08(9), N(3)−Ti−N(5) = 105.08(10), N(3)−Ti−N(6) = 94.22(10), N(2)−Ti−N(1) = 90.46(10), N(2)−Ti−N(4) = 101.99(10), N(3)−Ti−N(2) = 101.07(11), N(3)−Ti−N(4) = 94.55(10), N(2)−Ti−N(5) = 95.19(10).

Synthesis and Structural Characterization of Bis-(aminopyrolidinato)titanium Complexes. Upon reaction of the protioligands $HN^RN^{R'}$ with $Ti(NMe_2)_4$, complexes of the type $[Ti(N^RN^{R'})_2(NMe_2)_2]$ (**10**−**14**) were formed (Scheme 4). In accordance with the observations made with the amino-oxazoline ligand, these reactions were found to afford only the bis(amidinato) species, regardless of the stoichiometry employed, and complexes containing only a single amidinate ligand were found to be inaccessible.

Single crystals of the two complexes, **10** and **11**, containing the achiral ligands N^RN^H suitable for study by X-ray diffraction were prepared. Their structure analyses confirm the pseudo-octahedral structures depicted in Scheme 4 and are shown in Figures 7 and 8, respectively, along with principal bond lengths and angles. Interestingly, the molecular structures of **10** and **11** exhibit two different isomeric forms, which differ only in the rotation of the amidinate ligands. The orientation of the amidinate ligands in complex **10** is such that the two pyrroline ligands are mutually trans, with the N−Ar nitrogens trans to the NMe_2 ligands. This structure shows effective C_2 symmetry, with the two amidi-

(34) (a) Smrcina, M.; Major, P.; Majerovà, E.; Guerassina, T. A.; Eissenstat, M. A. *Tetrahedron* **1997**, *53*, 12867. (b) Ken, M. S.; Read de Alaniz, J.; Rovis T. *J. Org. Chem.* **2005**, *70*, 5725.
(35) Knight, R. L.; Leeper, F. J. *J. Chem. Soc., Perkin Trans. 1* **1998**, 1891.
(36) Charette, A. B.; Grenon, M. *Can. J. Chem.* **2001**, *79*, 1694.
(37) Charette, A. B.; Grenon, M. *Tetrahedron Lett.* **2000**, *41*, 1677.

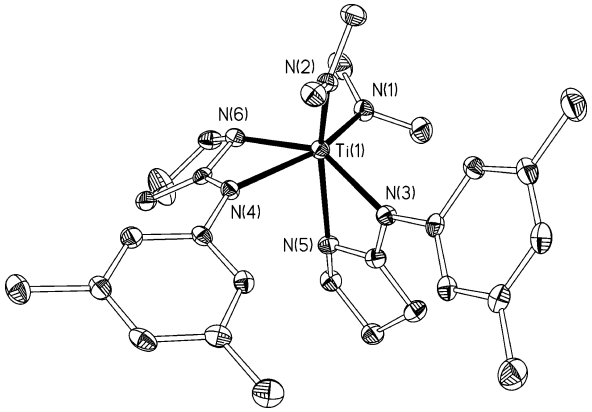

Figure 8. Molecular Structure of **11**. Thermal ellipsoids are drawn at 25% probability, and the H atoms have been omitted for clarity. Principal bond lengths (Å) and angles (deg): Ti(1)−N(1) = 1.908(3), Ti(1)−N(2) = 1.916(3), Ti(1)−N(3) = 2.080(3), Ti(1)−N(4) = 2.223(3), Ti(1)−N(5) = 2.275(3), Ti(1)−N(6) = 2.116(3), N(4)−Ti(1)−N(6) = 61.84(12), N(3)−Ti(1)−N(5) = 61.39(12), N(2)−Ti(1)−N(6) = 108.30(13), N(2)−Ti(1)−N(4) 91.46(12), N(2)−Ti(1)−N(1) = 99.47(15), N(2)−Ti(1)−N(3) = 97.38(13), N(1)−Ti(1)−N(6) = 91.92(13), N(1)−Ti(1)−N(3) = 104.67(13), N(1)−Ti(1)−N(5) = 93.68(13).

Scheme 5. Exchange Between the Two Isomers of Complex **11** in Solution

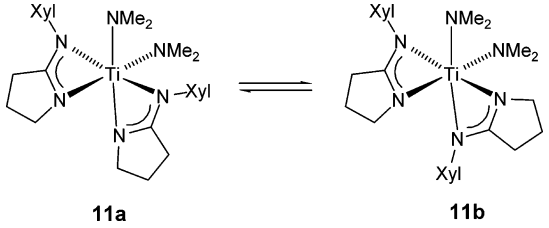

nate ligands occupying identical coordination sites within the molecular structure.

Conversely, the structure of **11** is such that one pyrroline nitrogen atom is trans to one of the NMe_2 ligands, with the other trans to the NAr nitrogen of the other amidinate ligand. The structure is therefore C_1 symmetric, with the amidinate ligands occupying different environments.

The NMR spectra for both complexes, **10** and **11**, are highly symmetrical at ambient temperature (295 K), which for complex **11**, is clearly inconsistent with the solid-state structure. However, the resonances broaden and decoalesce, upon cooling, indicating the presence of two isomers: a C_2-symmetric (**10a** and **11a**) and a C_1-symmetric (**10b** and **11b**) product in a 2:1 ratio. Analyses of the ROESY NMR spectra indicate that the two isomers, for both compounds, are the same as the two isomers obtained in the X-ray analyses. These data suggest that there is a rapid interconversion between **10a** and **10b** (and between **11a** and **11b**) on the NMR time scale via rotation of the amidinate ligands (Scheme 5).

A similar phenomenon is observed with the chiral derivatives $[Ti(N^{Ph}N^{Pr})(NMe_2)_2]$ (**12**) and $[Ti(N^{Xyl}N^{Pr})(NMe_2)_2]$ (**13**), but in these cases, the ^1H NMR spectra at ambient temperature are broad and only coalesce to afford time-averaged spectra at elevated temperatures. Like the achiral congeners, cooling of the samples yielded spectra consistent with a mixture of two isomers; this time however the two isomers were formed in equal proportions. Analyses of the ROESY NMR spectra indicated that the two isomers are completely analogous to the two diastereomers for **10** and **11**, namely, C_2-symmetric isomers **12a** and **13a** and C_1-symmetric isomers **12b** and **13b**.

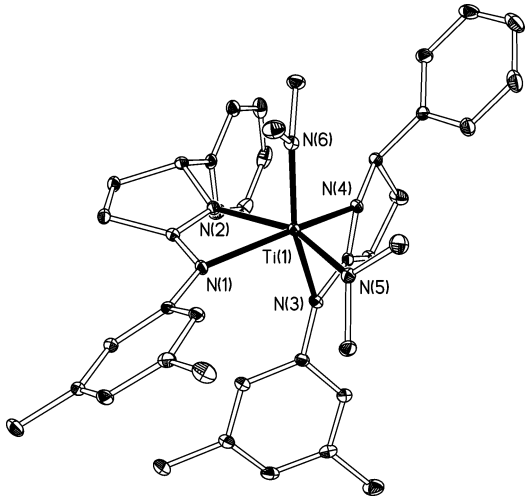

Figure 9. Molecular Structure of **14**. Thermal ellipsoids are drawn at 25% probability, and the H atoms have been omitted for clarity. Principal bond lengths (Å) and angles (deg): Ti(1)−N(1) = 2.107(2), Ti(1)−N(2) = 2.205(2), Ti(1)−N(3) = 2.219(2), Ti(1)−N(4) = 2.119(2), Ti(1)−N(5) = 1.911(2), Ti(1)−N(6) = 1.907(2), N(1)−Ti(1)−N(2) = 61.85(7), N(3)−Ti(1)−N(4) = 61.59(7), N(1)−Ti(1)−N(6) = 101.76(8), N(6)−Ti(1)−N(2) = 91.60(7), N(6)−Ti(1)−N(4) = 96.03(8), N(6)−Ti(1)−N(5) = 100.64(8), N(5)−Ti(1)−N(4) = 104.42(8), N(1)−Ti(1)−N(5) = 99.10(7), N(3)−Ti(1)−N(5) = 90.31(8).

The analogous reaction between racemic $HN^{Xyl}N^{Ph}$ (**9**) and $Ti(NMe_2)_4$ produced the expected bis(amide) complex $[Ti(N^{Xyl}N^{Ph})_2(NMe_2)_2]$ (**14**). In agreement with the data for complexes **10**−**13**, the NMR spectra at low temperature indicate the presence of two isomeric forms: the C_2-symmetric isomer **14a** and the C_1-symmetric isomer **14b**. Crystals suitable for X-ray diffraction were grown from diethyl ether at −30 °C. The molecular structure of complex **14**, with selected bond lengths and angles, is provided in Figure 9 and exhibits the same coordination geometry as those of **10** and **11**, with the structure occupying the C_1 isomeric form (**14b**).

Interestingly, although the structure contains both enantiomeric forms of the amidinate ligand, only the homochiral complex was isolated. Although this does not necessarily preclude the presence of the heterochiral species in solution, analysis of the low-temperature NMR spectra was inconclusive on this point, and the NMR spectra of the crystals were identical to NMR spectra of the bulk sample.

Analysis of the Chemical Exchange Between the Isomers of the Bis(amidinato)titanium Complexes. Activation parameters were determined on the basis of the NMe_2 ligand resonances in $[Ti(N^{Xyl}N^{H})_2(NMe_2)_2]$ (**11**), by measuring the line widths at half-height in the ^1H NMR spectra, at various temperatures between −84 and −68 °C. The line widths were measured using the line-fitting utility supplied with the Mestre-C NMR processing software and were corrected by subtracting the natural line width taken from the low-temperature spectrum. The observed rate coefficients were obtained from the line widths according to the expres-

Table 1. Activation Parameters for the Exchange of NMe_2 Ligands in $[Ti(N^{Xyl}N^{H})_2(NMe_2)_2]$ (**11**)

complex	$\Delta H^{\ddagger a}$	$\Delta S^{\ddagger b}$	$\Delta G^{\ddagger}_{298}{}^{a}$
11a	65(4)	120(15)	30(1)
11b (1)	71(5)	141(20)	29(2)
11b (2)	72(5)	143(20)	29(2)
mean	69(5)	135(20)	29(2)

[a] In kJ mol^{-1}. [b] In J mol^{-1} K^{-1}.

sion $k_{obs} = \pi\nu_{1/2,corr}$.[38] The observed rate coefficients were converted into the chemical rate coefficients, k_{chem}, by multiplying k_{obs} by the appropriate conversion factors for an AB_2 system, as described by Green et al.[39] These were subsequently used to construct Eyring plots for the determination of the activation parameters. The large positive activation entropy of ~130 J mol^{-1} K^{-1} is consistent with a dissociative mechanism for the amidinate rotation,[40] presumably via an initial decoordination of one of the amidinate nitrogen donors, followed by rotation and subsequent recoordination. The activation parameters are provided in Table 1, with the Eyring plots provided in the Supporting Information.

The experimental errors were estimated on the basis of the accuracy of the temperature measurement (±1 K) and that of the line width measurements [which was based on the digital resolution of the instrument (0.2 Hz)]. The sample was allowed to thermally equilibrate for at least 10 min at each temperature prior to data collection to ensure adequate temperature equilibration. A similar dynamic process was observed in the spectra of $[Ti(N^{Xyl}N^{Pr})_2(NMe_2)_2]$ (**13**) between −40 and 40 °C; however, in this case, the spectra were more complicated, and satisfactory kinetic analysis was not possible. Nevertheless, as indicated above, we assume that the dynamic process is similar to that observed for **11**.

Conclusions

We have shown that chiral amino-pyrroline ligands are readily accessible and offer excellent supporting environments for titanium. Moreover, these ligands possess a significant stability advantage over their oxazoline analogues because of their reduced propensity to undergo ring-opening decomposition reactions. Their assembly is modular which allows the rapid access of systems with varying ligand peripheries and thus different molecular shapes. Because of the universal applicability of the amidinate ligand, these new chiral ligands are thought to find applications in the field of organometallic chemistry and catalysis. Research toward this aim is currently under way in our laboratory.

Experimental Section

All manipulations of air- and moisture-sensitive species were performed under an atmosphere of argon or dinitrogen using standard Schlenk and glovebox techniques. Solvents were predried over activated 4 Å molecular sieves, dried over Na/K alloy (pentane, diethyl ether), Na (toluene), K (benzene, hexanes), or CaH_2 (dichloromethane), and distilled under argon prior to use. Deuterated solvents were dried over K (benzene-d_6, toluene-d_8) or CaH_2 (dichloromethane-d_2), vacuum distilled, and stored under dinitrogen in Teflon valve ampules. (*R*)-5-isopropylpyrrolidin-2-one was prepared from Boc-Ala-OH according to literature procedures.[34] All other reagents were purchased from commercial suppliers and used as received unless otherwise stated. Samples for NMR spectroscopy were prepared under dinitrogen in 5 mm Wilmad tubes equipped with J. Young Teflon valves. NMR spectra were recorded on Varian Unity Plus 400, Bruker Avance 200 or 300, or Bruker Avance II 400 FT-NMR spectrometers. NMR spectra are quoted in parts per million and were referenced internally relative to the residual protiosolvent (^{1}H) or solvent (^{13}C) resonances. Where necessary, NMR assignments were confirmed by the use of two-dimensional ^{1}H−^{1}H or ^{1}H−^{13}C correlation experiments or by ^{13}C DEPT experiments. Microanalyses were performed by the analytical services in the chemistry departments of the Université Louis Pasteur, Strasbourg, France, or the Universität Heidelberg, Germany. Mass spectra were recorded on a JEOL JMS 700 mass spectrometer by the mass spectrometry service at the Universität Heidelberg chemistry department.

2,6-Dimethylphenylamino-4(*S*)-isopropyloxazoline HNN_{ox} (H-1). A solution of 2,6-dimethylphenylisocyanate (1 equiv) in THF (50 mL) was added dropwise to a stirred solution of (*S*)-valinol (38.8 mmol) in dry THF (100 mL). The reaction mixture was left overnight at room temperature. The solvent was removed under reduced pressure, and the residue washed with pentane to afford (*S*)-1-hydroxy-2-[1-(2,6-dimethylurea)-3-methylbutane as a white powder which was used in the next step without further purification. A suspension of this intermediate in 150 mL of CH_2Cl_2 was cooled to 0 °C. Then 2.5 equiv (6.36 mL) of Et_3N were added, followed by 1.25 equiv (1.74 mL) of MsCl. After 5 min at 0 °C, the reaction mixture was allowed to reach room temperature, and this was followed by TLC. After 3 h, the reaction was complete. The mixture was washed with an aqueous solution of 5% NH_4Cl. The aqueous phase was extracted with CH_2Cl_2. The combined organic layers were dried over $MgSO_4$, filtered, and evaporated to dryness to afford a pale yellow oily solid. One hundred fifty milliliters of water/MeOH (1/1) and 40 mmol of NaOH (2.2 equiv) were added, and the resulting solution heated to reflux for 3 h. After it was cooled, the solution was concentrated, and brine (50 mL) was added. The aqueous solution was extracted 4× with CH_2Cl_2. The combined organic layers were dried over $MgSO_4$. After filtration and evaporation, the product was purified by column chromatography (1:1 EtOAc/pentane) to give the 2,6-dimethylphenylamino-4(*S*)-isopropyloxazoline in an 82% overall yield. ^{1}H NMR (300.1 MHz, $CDCl_3$, 293 K): δ 8.20 (1 H, br s, N*H*), 7.05 (2 H, m, CH_{meta}), 6.91 (1 H, m, CH_{para}), 4.35 (1 H, m, CH_{2oxa}), 4.03 (1 H, m, CH_{2oxa}), 3.58 (1 H, m, CH_{oxa}), 2.25 (6 H, s, CH_{3Ph}), 1.66 (1 H, m, CH^{i}Pr), 0.83 (6 H, d, CH_3 ^{i}Pr). ^{13}C{^{1}H} NMR (75.5 MHz, $CDCl_3$, 293 K): δ 155.7 (*C*═N), 144.3, 131.0 (*C*$_{ortho}$), 127.5 (*C*H$_{meta}$), 122.7 (*C*H$_{para}$), 70.4 (*C*H$_{2\ oxa}$), 60.9 (*C*H$_{oxa}$), 32.7 (*C*HMe$_2$), 18.3 (2 *C*H$_3$), 18.1 (CH*Me*$_2$), 17.8 (CH*Me*$_2$). Accurate mass FAB-MS for $[H_2NN_{ox}]^+$: *m*/*z* 233.1563 (calcd for $C_{14}H_{21}N_2O$ = 233.1654). Anal. Calcd for $C_{14}H_{20}N_2O$: C, 72.38; H, 8.68; N, 12.06. Found: C, 72.28; H, 8.63; N, 11.65.

$[Ti(NN_{ox})_2(NMe_2)_2]$ (2). A solution of HNN_{ox} (272 mg, 1.17 mmol, 2 equiv) in diethyl ether (20 mL) was added to a solution of $Ti(NMe_2)_4$ (131 mg, 0.59 mmol) in pentane (10 mL) at 0 °C, upon which the yellow solution immediately became bright red. The reaction was stirred at 0 °C for 5 min, and the volatiles were

(38) Sandström, J. *Dynamic NMR Spectroscopy*; Academic Press: New York, 1992.
(39) Green, M. L. H.; Wong, L.-L.; Sella, A. *Organometallics* **1992**, *11*, 2660.
(40) Stewart, P. J.; Blake, A. J.; Mountford, P. *Organometallics* **1998**, *17*, 3271.

removed under reduced pressure to afford **2** as an orange-red solid. Yield: 290 mg (83%). ^{1}H NMR (C_6D_6, 399.9 MHz, 293 K, this corresponds to the high-temperature limit): δ 7.11 (2 H, d, *m*-$C_6H_3Me_2$, ^3J = 6.4 Hz), 7.05 (2 H, d, *m*-$C_6H_3Me_2$, ^3J = 6.5 Hz), 6.97 (2 H, t, *p*-$C_6H_3Me_2$, ^3J = 7.4 Hz), 3.86 (4 H, s, C*H*$_2$CH^{i}Pr), 3.63 (2 H, s, C*H*^{i}Pr), 3.26 (12 H, s, NMe_2), 2.43 (6 H, s, $C_6H_3Me_2$), 2.11 (6 H, s, $C_6H_3Me_2$), 1.80 (2 H, m, C*H*Me_2), 0.85 (6 H, d, CHMe_2, ^3J = 6.5 Hz), 0.75 (6 H, d, CHMe_2, ^3J = 6.6 Hz). ^{13}C{^{1}H} NMR (C_7D_8, 100.6 MHz, 273 K): δ 164.6 (NCN), 145.5 (*ipso*-$C_6H_3Me_2$), 133.8 (*ortho*-$C_6H_3Me_2$), 129.6 (*meta*-$C_6H_3Me_2$), 128.5 (*meta*-$C_6H_3Me_2$), 123.9 (*para*-$C_6H_3Me_2$), 70.2 (CH_2O), 67.7 (C*H*^{i}Pr), 48.1 (NMe_2), 34.2 (C*H*Me_2), 19.9 (CH*Me*$_2$), 19.7 (CH*Me*$_2$), 19.4 ($C_6H_3Me_2$), 17.3 ($C_6H_3Me_2$).

[Ti(NN$_{ox}$){κ^3-N(2,6-$C_6H_3Me_2$)C(NMe_2)NC(^{i}Pr)CH_2O}-(NMe_2)] (3). A Schlenk tube was charged with 1 equiv of Ti(NMe_2)$_4$ (0.6 mmol) and 2 equiv of HNN$_{ox}$ **(H-2)** (1.2 mmol). Toluene (2 mL) was added to this mixture, and the resulting red solution was stirred for 1 h. The volatiles were removed under reduced pressure, and pentane was added to dissolve the residue (~2 mL). The solution was cooled to −20 °C, and yellow crystals were obtained after several weeks. ^{1}H NMR (C_6D_6, 399.9 MHz, 293 K): δ 7.12−6.91 (6 H, overlapping m, $C_6H_3Me_2$), 5.26 (1 H, dd, C*H*HO, ^2J = 10.0 Hz, ^3J = 5.4 Hz), 4.51 (1 H, d, CH*H*O, ^2J = 10.0 Hz), 3.84−3.67 (4 H, overlapping m, CH^{i}Pr, oxazoline CH_2 and CH), 3.08 (6 H, s, Ti−NMe_2), 2.53 (3 H, s, $C_6H_3Me_2$), 2.42 (3 H, s, $C_6H_3Me_2$), 2.24 (3 H, s, $C_6H_3Me_2$), 2.09 (6 H, br. s, $NCNMe_2$ and C*H*Me_2), 1.94 (3 H, s, $C_6H_3Me_2$), 1.67 (1 H, m, C*H*Me_2), 0.92 (3 H, d, CH*Me*$_2$, ^3J = 6.8 Hz), 0.77 (3 H, d, CH*Me*$_2$, ^3J = 6.5 Hz), 0.75 (3 H, d, CH*Me*$_2$, ^3J = 6.8 Hz), 0.64 (3 H, d, CH*Me*$_2$, ^3J = 6.7 Hz). MS (EI): *m*/*z* = 554.3 [M − NMe_2]$^+$. Anal. Calcd for $C_{32}H_{50}N_6O_2Ti$: C, 64.20; H, 8.42; N, 14.04. Found: C, 63.85; H, 8.69; N, 14.13.

[Ti{κ^3-N(2,6-$C_6H_3Me_2$)C(NMe_2)NC(^{i}Pr)CH_2O}$_2$] (4). [Ti(N-N$_{ox}$){κ^3-N(3,5-$C_6H_3Me_2$)C(NMe_2)NC(^{i}Pr)CH_2O}(NMe_2)] (**2**) was dissolved in benzene and heated to 70 °C for 2 h. The solvent was removed under reduced pressure to afford **4** as a yellow solid. Yield: 74%. Crystals suitable for X-ray diffraction were grown by slow concentration of a saturated solution in benzene. NMR spectroscopy indicated the presence of two interchanging isomers: a = major isomer and b = minor isomer. ^{1}H NMR data (399.9 MHz, CD_2Cl_2, 263 K): δ 7.01 (2 H, d, *m*-$C_6H_3Me_2$ {a}, ^3J = 7.1 Hz), 6.92 (2 H, d, *m*-$C_6H_3Me_2$ {a}, ^3J = 7.0 Hz), 6.87 (2 H, overlapping m, *p*-$C_6H_3Me_2$ {a}; 4 H, overlapping m, *o*-$C_6H_3Me_2$ {b}), 6.75 (2 H, t, *p*-$C_6H_3Me_2$ {b}, ^3J = 7.4 Hz), 4.47 (2 H, dd, C*H*HO {a}, ^2J = 10.5 Hz, ^3J = 6.2 Hz), 4.05 (2 H, dd, CH*H*O {a}, ^2J = 10.5 Hz, ^3J = 1.7 Hz), 3.91 (2 H, d, C*H*HO {b}, ^2J = 10.1 Hz), 3.79 (2 H, apparent t, CH*H*O {b}, apparent J = 5.9 Hz), 3.67 (2 H, apparent t, C*H*^{i}Pr {b}, apparent J = 5.1 Hz), 2.99 (2 H, apparent t, C*H*^{i}Pr {a}, apparent J = 7.1 Hz), 2.61 (2 H, m, C*H*Me_2 {b}), 2.48 (12 H, s, NMe_2 {a}; 12 H, s, NMe_2 {b}), 2.45 (6 H, s, $C_6H_3Me_2$ {a}), 2.16 (6 H, s, $C_6H_3Me_2$ {b}), 2.10 (6 H, s, $C_6H_3Me_2$ {b}), 2.01 (6 H, s, $C_6H_3Me_2$ {a}), 1.07 (6 H, d, CHMe_2 {b}, ^3J = 6.7 Hz), 0.89 (6 H, d, CHMe_2 {b}, ^3J = 6.9 Hz), 0.59−0.50 (8 H, overlapping m, CHMe_2 {a} and C*H*Me_2 {a}), 0.41 (6 H, d, CHMe_2 {a}, ^3J = 5.9 Hz). ^{13}C{^{1}H} NMR (100.6 MHz, CD_2Cl_2, 263 K): δ 172.1 (C═N {a}), 166.4 (C═N {b}), 147.0 (*ipso*-$C_6H_3Me_2$ {b}), 146.5 (*ipso*-$C_6H_3Me_2$ {a}), 134.0 (*o*-$C_6H_3Me_2$ {a}), 133.3 (*o*-$C_6H_3Me_2$ {b}), 132.9 (*o*-$C_6H_3Me_2$ {b}), 132.8 (*o*-$C_6H_3Me_2$ {a}), 128.1 (*m*-$C_6H_3Me_2$ {b}), 127.9 (*m*-$C_6H_3Me_2$ {a}), 127.8 (*m*-$C_6H_3Me_2$ {a}), 127.6 (*m*-$C_6H_3Me_2$ {b}), 123.5 (*p*-$C_6H_3Me_2$ {a}), 121.9 (*p*-$C_6H_3Me_2$ {b}), 79.3 (CH_2O {a}), 73.5 (CH_2O {b}), 72.4 (C*H*^{i}Pr {a}), 69.3 (C*H*^{i}Pr {b}), 38.4 (NMe_2 {a}), 37.6 (NMe_2 {b}), 34.4 (C*H*Me_2 {b}), 31.2 (C*H*Me_2 {a}), 21.0 (CH*Me*$_2$ {a}), 20.8 (CH*Me*$_2$ {b}), 20.1 (CH*Me*$_2$ {a}), 19.1 ($C_6H_3Me_2$ {a}), 18.5 ($C_6H_3Me_2$ {a} and {b}), 18.3 ($C_6H_3Me_2$ {b}), 17.2 (CH*Me*$_2$ {b}). Anal. Calcd for $C_{32}H_{50}N_6O_2Ti$: C, 64.20; H, 8.42; N, 14.04. Found: C, 63.88; H, 8.41; N, 13.63.

General Procedure for the Synthesis of Amidines HN^{R}N$^{R'}$. Tf_2O (1.2 equiv) was slowly added dropwise to a solution of pyrrolidin-2-one and pyridine (3 equiv) in CH_2Cl_2 at −40 °C. The mixture was allowed to warm to 0 °C over 3 h. After the mixture was cooled to −40 °C, 3 equiv of arylamine were introduced in one portion. The reaction was then slowly warmed to room temperature and stirred overnight. CH_2Cl_2 was added, and the organic phase was washed three times with NaOH (1 M). The aqueous layers were extracted with CH_2Cl_2, and the combined organic layers were dried over Na_2SO_4 and concentrated under reduced pressure. Purification by column chromatography (EtOAc/pentane) gave the pure product in a 45−50% yield.

2-(Phenylimino)pyrroline (HN^{Ph}N^H) (H-5). ^{1}H NMR (300.1 MHz, $CDCl_3$, 293 K): δ 7.26 (2 H, m, C*H*$_{ortho}$), 7.01 (2 H, m, C*H*$_{meta}$), 6.94 (2 H, m, C*H*$_{para}$), 5.05 (1 H, br s, N*H*), 3.41 (2 H, t, C*H*$_2$, ^3J = 6.8 Hz), 2.48 (2 H, t, C*H*$_2$, ^3J = 7.9 Hz), 1.97 (2 H, m, C*H*$_2$). ^{13}C{^{1}H} NMR (75.5 MHz, $CDCl_3$, 293 K): δ 164.2, 148.9, 129.0 (*C*H$_{meta}$), 122.2 (*C*H$_{para}$), 121.4 (*C*H$_{ortho}$), 47.3 (*C*H$_2$), 30.4 (*C*H$_2$), 22.3 (*C*H$_2$). MS (FAB): *m*/*z* 231.1 (M + H)$^+$. Anal. Calcd for $C_{10}H_{12}N_2$: C, 74.97; H, 7.55; N, 17.48. Found: C, 74.77; H, 7.41; N, 17.72.

2-(3,5-Dimethylphenylimino)pyrroline (HN^{Xyl}N^H) (H-6). ^{1}H NMR (300.1 MHz, $CDCl_3$, 293 K): δ 6.67 (2 H, s, C*H*$_{ortho}$), 6.64 (1 H, s, C*H*$_{para}$), 4.62 (1 H, br s, N*H*), 3.47 (2 H, t, C*H*$_2$, ^3J = 6.8 Hz), 2.54 (2 H, t, C*H*$_2$, ^3J = 8.0 Hz), 2.27 (6 H, s, C*H*$_3$), 2.03 (2 H, m, C*H*$_2$). ^{13}C{^{1}H} NMR (75.5 MHz, $CDCl_3$, 293 K): δ 163.7, 148.4, 138.7, 124.2 (*C*H$_{para}$), 119.0 (*C*H$_{ortho}$), 47.4 (*C*H$_2$), 30.7 (*C*H$_2$), 22.2 (*C*H$_2$), 21.4 (*C*H$_3$). MS (FAB): *m*/*z* 189.0 (M + H)$^+$. Anal. Calcd for $C_{12}H_{16}N_2$: C, 76.55; H, 8.57; N, 14.88. Found: C, 75.91; H, 8.56; N, 14.78.

2-(Phenylimino)-5-isopropylpyrroline (HN^{Ph}N^{Pr}) (H-7). ^{1}H NMR (300.1 MHz, $CDCl_3$, 293 K): δ 7.22 (2 H, m, C*H*$_{Ph}$), 6.94 (3 H, m, C*H*$_{Ph}$), 5.20 (1 H, br s, N*H*), 3.34 (1 H, q, C*H*$_{pyrr}$, ^3J = 6.9 Hz), 2.45 (2 H, m, C*H*$_{2\ pyrr}$), 2.01 (1 H, m, C*H*Me_2), 1.59 (2 H, m, C*H*$_{2\ pyrr}$), 0.85 (3 H, d, C*H*$_3$, ^3J = 6.8 Hz), 0.83 (3 H, d, C*H*$_3$, ^3J = 6.8 Hz). ^{13}C{^{1}H} NMR (75.5 MHz, $CDCl_3$, 293 K): δ 163.7 (*C*═N), 149.7 (C$_{Ph}$), 129.1 (CH$_{Ph}$), 122.3 (CH$_{Phpara}$), 121.9 (CH$_{Ph}$), 63.9 (CH), 33.6 (CH), 29.8 (CH_2), 25.6 (CH_2), 19.2 (CH_3), 18.3 (CH_3). MS (ES): *m*/*z* 203.158 (M + H)$^+$. Anal. Calcd for $C_{13}H_{18}N_2$: C, 77.18; H, 8.97; N, 13.85. Found: C, 76.73; H, 8.97; N, 13.53.

2-(3,5-Dimethylphenylimino)-5-isopropylpyrroline (HN^{Xyl}N^{Pr}) (H-8). ^{1}H NMR (300.1 MHz, $CDCl_3$, 293 K): δ 6.63 (1 H, s, C*H*$_{para}$), 6.60 (2 H, s, C*H*$_{ortho}$), 5.47 (1 H, br s, N*H*), 3.35 (1 H, q, C*H*$_{pyrr}$, ^3J = 6.8 Hz), 2.46 (2 H, m, C*H*$_{2pyrr}$), 2.24 (6 H, s, C*H*$_{3Ph}$), 2.01 (1 H, m, C*H*$_2$), 1.69 (1 H, m, C*H*$_2$), 1.60 (1 H, m, C*H*Me_2), 0.88 (3 H, d, C*H*$_3$, ^3J = 6.7 Hz), 0.84 (3 H, d, C*H*$_3$, ^3J = 6.7 Hz). ^{13}C{^{1}H} NMR (75.5 MHz, $CDCl_3$, 293 K): δ 163.2, 149.7, 138.6, 124.1 (*C*H$_{para}$), 119.4 (*C*H$_{ortho}$), 63.9 (*C*H$_{pyrr}$), 33.5 (*C*H$_{pyrr}$), 29.9 (*C*H$_2$), 25.6 (*C*H$_2$), 21.4 (*C*H$_{3Ph}$), 19.2 (*C*H$_{3^iPr}$), 18.3 (CH$_{3^iPr}$). MS (ES): *m*/*z* 231.188 (M + H)$^+$. Anal. Calcd for $C_{15}H_{22}N_2$: C, 78.21; H, 9.63; N, 12.16. Found: C, 77.83; H, 9.61; N, 11.88.

2-(3,5-Dimethylphenylimino)-5-phenylpyrroline (HN^{Xyl}N^{Ph}) (H-9). ^{1}H NMR (399.9 MHz, $CDCl_3$, 293 K): δ 7.30−7.18 (5 H, overlapping m, Ph), 6.62 (2 H, s, *o*-$C_6H_3Me_2$), 6.57 (1 H, s, *p*-$C_6H_3Me_2$), 4.71 (1 H, broad m, NC*H*Ph), 2.67−2.51 (2 H, overlapping m, C*H*$_2$), 2.44−2.35 (1 H, overlapping m, C*H*$_2$), 2.20 (6 H, s, $C_6H_3Me_2$), 1.87−1.77 (1 H, overlapping m, C*H*$_2$). ^{13}C{^{1}H} NMR (100.6 MHz, $CDCl_3$ 293 K): 171.3 (C═N) δ 143.8 (*ipso*-Ph), 142.0 (*ipso*-$C_6H_3Me_2$) 138.7 (*meta*-$C_6H_3Me_2$), 128.6 (Ph), 127.5 (Ph),

125.9 (Ph), 124.2 (*p*-$C_6H_3Me_2$), 119.0 (*o*-$C_6H_3Me_2$), 62.1 (broad, N*C*HPh), 32.4 (CH_2), 30.1 (broad, CH_2), 21.4 ($C_6H_3Me_2$). Accurate high-resolution mass FAB-MS for $[H_2N^{Xyl}N^{Ph}]^+$: *m*/*z* 265.1717 (calcd for $C_{18}H_{21}N_2 = 265.1705$). Anal. Calcd for $C_{18}H_{20}N_2 \cdot 0.25CH_2Cl_2$: C, 76.75; H, 7.23; N, 9.81. Found: C, 76.09; H, 7.55; N, 9.26.

General Procedure for the Preparation of $[Ti(N^RN^{R'})_2(NMe_2)_2]$. In the glovebox, a Schlenk tube was charged with $Ti(NMe_2)_4$ (~0.5 mmol) and dissolved in toluene (10 mL). The solution was cooled to 0 °C for the dropwise addition of the appropriate amidinate ligand (2 equiv) in toluene (10 mL). The solution was allowed to warm to ambient temperature and stirred for a further 30 min. The volatile components were removed under reduced pressure to afford the desired compounds as brown solids (**10**, **11**, and **13**) or a brown oil (**12**).

$[Ti(N^{Ph}N^H)_2(NMe_2)_2]$ (10). Yield: 65%. ^{1}H NMR (399.9 MHz, CD_2Cl_2): δ (293 K) 7.18 (4 H, m, *m*-Ph), 6.86 (6 H, overlapping m, *o*-Ph, *p*-Ph), 3.77 (4 H, t, NCH_2, $^3J = 6.9$ Hz), 3.35 (12 H, s, NMe_2), 2.55 (4 H, t, $^3J = 8.0$ Hz, $NCCH_2$), 1.96 (4 H, m, NCH_2CH_2); (183 K) 7.32 (1 H, br. m, Ph), 7.13 (3 H, br. s, Ph), 7.04 (1 H, br. d, Ph), 6.96 (1 H, br. m, Ph), 6.73 (4 H, br. m, Ph), 4.08−1.63 (12 H, overlapping m, CH_2), 3.39 (3 H, s, NMe_2 {asym}), 3.29 (6 H, s, NMe_2 {sym}), 3.10 (3 H, s, NMe_2 {asym}). $^{13}C\{^1H\}$ NMR (100.6 MHz, CD_2Cl_2, 183 K): δ 176.9 (NCN), 176.8 (NCN), 176.1 (NCN), 147.8 (*ipso*-Ph), 147.5 (*ipso*-Ph), 128.5 (Ph), 128.3 (Ph), 128.2 (Ph), 120.1 (Ph), 119.8 (Ph), 119.3 (Ph), 118.9 Ph), 51.4 (CH_2), 51.0 (CH_2), 50.9 (CH_2), 46.7 (NMe_2 {asym}), 45.9 (NMe_2 {sym}), 45.9 (NMe_2 {asym}), 31.3 (CH_2), 29.7 (CH_2), 29.4 (CH_2), 24.3 (CH_2), 23.9 (CH_2), 22.6 (CH_2). Anal. Calcd for $C_{24}H_{34}N_6Ti$: C, 63.43; H, 7.54; N, 18.49. Found: C, 62.88; H, 7.55; N, 18.11.

$[Ti(N^{Xyl}N^H)_2(NMe_2)_2]$ (11). Yield: 70%. ^{1}H NMR (399.9 MHz, CD_2Cl_2): δ (293 K) 6.52 (2 H, s, *p*-$C_6H_3Me_2$), 6.49 (4 H, s, *o*-$C_6H_3Me_2$), 3.77 (4 H, t, NCH_2, $^3J = 6.9$ Hz), 3.33 (12 H, s, NMe_2), 2.57 (4 H, t, N=CCH_2, $^3J = 8.0$ Hz), 2.23 (12 H, s, $C_6H_3Me_2$), 1.97 (4 H, quin, NCH_2CH_2, $^3J = 7.7$ Hz); (183 K) 6.70 (1 H, s, *p*-$C_6H_3Me_2$ {asym}), 6.68 (2 H, s, *o*-$C_6H_3Me_2$ {asym}), 6.48 (1 H, s, *p*-$C_6H_3Me_2$ {asym}), 6.45 (2 H, s, *p*-$C_6H_3Me_2$ {sym}), 6.40 (2 H, s, *o*-$C_6H_3Me_2$ {asym}), 6.37 (4 H, s, *o*-$C_6H_3Me_2$ {sym}), 4.10−1.74 (6 H {sym} + 6 H {asym}, overlapping m, CH_2), 3.40 (6 H, s, NMe_2 {asym}), 3.28 (12 H, s, NMe_2 {sym}), 3.10 (6 H, s, NMe_2 {asym}), 2.34 (6 H, s, $C_6H_3Me_2$ {asym}), 2.20 (12 H, s, $C_6H_3Me_2$ {sym}), 2.17 (6 H, s, $C_6H_3Me_2$ {asym}). $^{13}C\{^1H\}$ NMR (100.6 MHz, CD_2Cl_2, 183 K): δ 177.0 (NCN), 176.6 (NCN), 176.4 (NCN), 147.8 (*ipso*-$C_6H_3Me_2$), 147.5 (*ipso*-$C_6H_3Me_2$), 147.2 (*ipso*-$C_6H_3Me_2$), 137.7 (*m*-$C_6H_3Me_2$ {asym}), 137.6 (*m*-$C_6H_3Me_2$ {sym}), 137.5 (*m*-$C_6H_3Me_2$ {asym}), 122.1 (*p*-$C_6H_3Me_2$ {asym}), 121.0 (*p*-$C_6H_3Me_2$ {sym}), 120.8 (*p*-$C_6H_3Me_2$ {asym}), 118.0 (*o*-$C_6H_3Me_2$ {asym}), 117.5 (*o*-$C_6H_3Me_2$ {overlapping sym, asym}), 51.6 (CH_2), 51.1 (CH_2), 50.7 (CH_2), 47.2 (NMe_2 {asym}), 45.8 (NMe_2 {sym}), 45.5 (NMe_2 {asym}), 31.1 (CH_2), 29.7 (CH_2), 29.6 (CH_2), 24.1 (CH_2), 23.8 (CH_2), 22.6 (CH_2), 21.2 ($C_6H_3Me_2$ {asym}), 21.1 ($C_6H_3Me_2$ {sym}), 21.0 ($C_6H_3Me_2$ {asym}). Anal. Calcd for $C_{26}H_{42}N_6Ti$: C, 64.19; H, 8.70; N, 17.27. Found: C, 64.66; H, 8.21; N, 16.69.

$[Ti(N^{Ph}N^{Pr})_2(NMe_2)_2]$ (12). Yield: 75%. ^{1}H (399.9 MHz, CD_2Cl_2, 223 K): δ 7.28 (2 H, t, *m*-Ph {asym}, $^3J = 7.9$ Hz), 7.15−7.03 (5 H, overlapping m, Ph), 6.93 (2 H, d, *o*-Ph {asym}, $^3J = 7.6$ Hz), 6.85 (1 H, t, *p*-Ph {asym}, $^3J = 7.3$ Hz), 6.80−6.73 (10 H, overlapping m, Ph), 4.18 (2 H {sym} + 2 H {asym}, m, C*H*^{i}Pr), 3.63−1.71 (16 H, overlapping m, CH_2), 3.34 (6 H, s, NMe_2 {asym}), 3.30 (12 H, s, NMe_2 {sym}), 3.09 (6 H, s, NMe_2 {asym}), 1.96 (2 H, m, C*H*Me_2), 1.57 (2 H, m, C*H*Me_2), 0.94 (6 H, d, CH*Me*$_2$ {sym}, $^3J = 6.9$ Hz), 0.95 (3 H, d, CH*Me*$_2$ {asym}, $^3J = 6.8$ Hz), 0.78 (6 H {sym} + 6 H {asym}, overlapping m, CH*Me*$_2$), 0.73 (3 H, d, CH*Me*$_2$ {asym}, $^3J = 6.7$ Hz). $^{13}C\{^1H\}$ NMR (100.6 MHz, CD_2Cl_2, 223 K): δ 176.0 (NCN {sym}), 174.9 (NCN {asym}), 173.8 (NCN {asym}), 148.7 (*ipso*-Ph {sym}), 148.5 (*ipso*-Ph {asym}), 148.3 (*ipso*-Ph {asym}), 128.5 (*m*-Ph {asym}), 128.4 (*m*-Ph {sym}), 128.3 (*m*-Ph {asym}), 121.3 (*p*-Ph {asym}), 120.7 (*p*-Ph {sym}), 120.4 (*p*-Ph {asym}), 119.5 (*o*-Ph {sym}), 119.1 (*o*-Ph {asym, overlapping}), 70.1 (*C*H^{i}Pr {asym}), 67.8 (*C*H^{i}Pr {sym}), 67.6 (*C*H^{i}Pr {asym}), 47.0 (NMe_2 {asym}), 46.4 (NMe_2 {sym}), 45.8 (NMe_2 {asym}), 34.1 (*C*HMe_2 {asym}), 34.0 (*C*HMe_2 {sym}), 33.5 (*C*HMe_2 {asym}), 30.5 (CH_2), 30.2 (CH_2), 30.0 (CH_2), 25.4 (CH*Me*$_2$ {asym}), 24.0 (CH*Me*$_2$ {sym}), 23.3 (CH*Me*$_2$ {asym}), 19.0 (CH_2), 18.7 (CH_2), 18.3 (CH_2). Accurate mass EI-MS for $[Ti(N^{Ph}N^{Pr})(NMe_2)]^+$: *m*/*z* 494.2752 (calcd for $C_{28}H_{40}N_5Ti = 494.2763$). For $[Ti(N^{Ph}N^{Pr})]^+$: *m*/*z* 450.2268 (calcd for $C_{26}H_{34}N_4Ti = 450.2263$). Anal. Calcd for $C_{30}H_{46}N_6Ti$: C, 66.90; H, 8.61; N, 15.60. Found: C, 66.99; H, 8.46; N, 15.12.

$[Ti(N^{Xyl}N^{Pr})_2(NMe_2)_2]$ (13). Yield: 59%. ^{1}H NMR (399.9 MHz, CD_2Cl_2, 233 K): δ 6.64 (2 H, s, *o*-$C_6H_3Me_2$ {asym}), 6.59 (1 H, s, *p*-$C_6H_3Me_2$ {asym}), 6.47 (2 H, s, *p*-$C_6H_3Me_2$ {sym}), 6.45 (2 H, s, *o*-$C_6H_3Me_2$ {asym}), 6.41 (1 H, s, *p*-$C_6H_3Me_2$ {asym}), 6.38 (4 H, s, *o*-$C_6H_3Me_2$ {sym}), 4.22−2.32 (6 H {sym} + 6 H {asym}, overlapping m, CH_2 and C*H*^{i}Pr), 3.32 (6 H, s, NMe_2 {asym}), 3.26 (12 H, s, NMe_2 {sym}), 3.01 (6 H, s, NMe_2 {asym}), 2.29 (6 H, s, $C_6H_3Me_2$ {asym}), 2.18 (12 H, s, $C_6H_3Me_2$ {sym}), 2.16 (6 H, s, $C_6H_3Me_2$ {asym}), 1.97 (4 H, s, CH_2 {sym}), 1.86 (2 H, s, CH_2 {asym}), 1.57 (2 H, s, CH_2 {asym}), 0.97 (6 H {sym} + 3 H {asym}, d, CH*Me*$_2$, $^3J = 6.9$ Hz), 0.94 (3 H, d, CH*Me*$_2$ {asym}, $^3J = 6.9$ Hz), 0.80 (6 H {sym} + 3 H {asym}, d, CH*Me*$_2$, $^3J = 6.9$ Hz), 0.76 (3 H, d, CH*Me*$_2$ {asym}, $^3J = 6.9$ Hz). $^{13}C\{^1H\}$ NMR (100.6 MHz, CD_2Cl_2, 233 K): δ 175.8 (NCN {sym}), 175.0 (NCN {asym}), 173.5 (NCN {asym}), 148.6 (*ipso*-$C_6H_3Me_2$ {sym}), 148.4 (*ipso*-$C_6H_3Me_2$ {asym}), 148.0 (*ipso*-$C_6H_3Me_2$ {asym}), 137.8 (*m*-$C_6H_3Me_2$ {sym}), 137.7 (*m*-$C_6H_3Me_2$ {asym}), 137.6 (*m*-$C_6H_3Me_2$ {asym}), 122.1 (*p*-$C_6H_3Me_2$ {asym}), 121.3 (*p*-$C_6H_3Me_2$ {sym}), 121.2 (*p*-$C_6H_3Me_2$ {asym}), 119.3 (*o*-$C_6H_3Me_2$ {asym}), 118.4 (*o*-$C_6H_3Me_2$ {asym}), 118.3 (*o*-$C_6H_3Me_2$ {sym}), 71.2 (*C*H^{i}Pr), 67.8 (*C*H^{i}Pr), 67.5 (*C*H^{i}Pr), 47.3 (NMe_2 {asym}), 46.3 (NMe_2 {sym}), 45.8 (NMe_2 {asym}), 34.2 (*C*HMe_2 {asym}), 34.1 (*C*HMe_2 {sym}), 33.8 (*C*HMe_2 {asym}), 30.6 (CH_2), 30.4 (CH_2), 30.1 (CH_2), 25.8 (CH*Me*$_2$ {asym}), 23.7 (CH*Me*$_2$ {sym}), 23.5 (CH*Me*$_2$ {asym}), 21.5 ($C_6H_3Me_2$ {asym}), 21.4 ($C_6H_3Me_2$ {sym}), 21.3 ($C_6H_3Me_2$ {asym}), 19.0 (CH_2 {sym}), 18.6 (CH_2 {asym}), 18.3 (CH_2 {asym}). Anal. Calcd for $C_{34}H_{54}N_6Ti$: C, 68.67; H, 9.15; N, 14.13. Found: C, 68.30; H, 8.73; N, 13.59.

$[Ti(N^{xyl}N^{Ph})_2(NMe_2)_2]$ (14). Yield: 51%. ^{1}H NMR (399.9 MHz, CD_2Cl_2, 203 K): δ 7.45−7.09 (10 H + 10 H, overlapping m, Ph {asym} + {sym}), 6.83−6.43 (6 H + 6H, overlapping m, $C_6H_3Me_2$ {asym} + {sym}), 5.29−5.28 (2 H, overlapping m, NC*H*Ph {sym}), 4.8−4.63 (2 H, overlapping m, NC*H*Ph {asym}), 3.13 (6 H, s, NMe_2 {asym}), 3.08 (6 H, s, NMe_2 {asym}), 2.98 (12 H, s, NMe_2 {sym}), 3.22−1.52 (8 H {asym} + 8 H {sym}, overlapping m, CH_2), 2.29 (6 H, s, $C_6H_3Me_2$ {asym}), 2.20 (12 H, s, $C_6H_3Me_2$ {sym}), 2.17 (6 H, s, $C_6H_3Me_2$ {asym}). $^{13}C\{^1H\}$ NMR (100.6 MHz, CD_2Cl_2, 203 K): δ 176.6 (NCN), 175.6 (NCN), 174.6 (NCN), 147.8 (*ipso*-$C_6H_3Me_2$), 147.7 (*ipso*-$C_6H_3Me_2$), 147.2 (*ipso*-$C_6H_3Me_2$), 146.3 (*ipso*-Ph), 146.1 (*ipso*-Ph), 145.6 (*ipso*-Ph), 137.7 (*m*-$C_6H_3Me_2$ {asym}), 137.7 (*m*-$C_6H_3Me_2$ {sym}), 137.5 (*m*-$C_6H_3Me_2$ {asym}), 127.6 (*m*-Ph), 127.6 (*m*-Ph), 127.5 (*m*-Ph), 126.1 (*p*-Ph), 126.1 (*p*-Ph), 126.0 (*p*-Ph), 125.8 (*o*-Ph), 125.7 (*o*-Ph), 125.6 (*o*-Ph), 122.2 (*p*-$C_6H_3Me_2$), 121.6 (*p*-$C_6H_3Me_2$), 121.3 (*p*-$C_6H_3Me_2$), 119.0 (*o*-$C_6H_3Me_2$), 118.2 (*o*-$C_6H_3Me_2$), 117, 9 (*o*-$C_6H_3Me_2$), 67.6

Table 2. X-ray Data for **3**, **4**·C_6H_6, **10**, **11**, and **14**

	3	**4**·C_6H_6	**10**	**11**	**14**
empirical formula	$C_{32}H_{50}N_6O_2Ti$	$C_{38}H_{56}N_6O_2Ti$	$C_{24}H_{34}N_6Ti$	$C_{28}H_{42}N_6Ti$	$C_{40}H_{50}N_6Ti$
fw	598.68	676.80	454.47	510.58	662.78
cryst size (mm)	0.10 × 0.09 × 0.07	0.07 × 0.05 × 0.05	0.10 × 0.10 × 0.10	0.10 × 0.10 × 0.10	0.25 × 0.25 × 0.25
cryst syst	monoclinic	monoclinic	monoclinic	monoclinic	monoclinic
space group	$P2_1$	$P2_1$	$P2_1/a$	$P2_1/n$	Cc
a (Å)	9.502(5)	11.8179(8)	8.605(5)	15.9730(5)	21.222(3)
b (Å)	16.326(5)	12.6276(9)	16.710(5)	8.2490(3)	12.140(2)
c (Å)	10.807(5)	12.8169(9)	16.677(5)	22.5880(10)	15.759(2)
α (deg)	90	90	90	90	90
β (deg)	94.00(5)	98.651	93.63(5)	110.315(2)	117.311(2)
γ (deg)	90	90	90	90	90
V (Å^3)	1672.4(13)	1890.9(2)	2393(2)	2791.1(2)	3607.4(8)
Z	2	2	4	4	4
D_c (Mg m^{-3})	1.189	1.189	1.261	1.215	1.220
μ (mm^{-1})	0.292	0.266	0.380	0.333	0.274
max. and min. trans	0.985, 0.968	0.984, 0.980	0.966, 0.959	0.969, 0.965	0.936, 0.927
index ranges (*hkl*)	−13 to 8	−14 to 13	−7 to 12	−15 to 17	−31 to 31
	−20 to 22	−14 to 14	−21 to 23	−10 to 10	0 to 18
	−15 to 15	0 to 15	−23 to 19	−29 to 29	−23 to 22
θ (deg)	1.0−30.0	1.6−25.0	1.0−30.0	1.0−27.5	1.0−32.1
T (K)	173(2)	100(2)	173(2)	173(2)	100(2)
F(000)	644	728	968	1096	1416
reflns collected	14 513	43 494	22 453	9818	45 209
reflns indep [R_{int}]	8834 [0.0492]	6671 [0.0765]	6979 [0.0826]	6325 [0.1001]	11 667 [0.038]
data/restraints/params	8834/1/370	6671/1/425	6979/0/280	5825/0/316	11 667/2/425
GOF on F^2	1.009	0.985	1.180	0.921	0.9033
Final R indices	$R_1 = 0.0662$	$R_1 = 0.0471$	$R_1 = 01008$	$R_1 = 0.0645$	$R = 0.0402$
[$I > 2\sigma(I)$]	$R_2 = 0.1299$	$R_2 = 0.1012$	$R_2 = 0.1524$	$R_2 = 0.1440$	$R2 = 0.0938$
R indices	$R_1 = 0.102$	$R_1 = 0.0640$	$R_1 = 0.1726$	$R_1 = 0.1823$	$R = 0.0600$
(all data)	$R_2 = 0.1634$	$R_2 = 0.1129$	$R_2 = 0.1724$	$R_2 = 0.1871$	$R2 = 0.1186$
absolute struct params	0.03(3)	−0.01(3)			0.239(18)
largest residual peak (e Å^{-3})	0.57 and −0.62	0.34 and −0.51	0.46 and −0.57	0.33 and −0.44	0.61 and −1.07

(NCHPh {asym}), 65.4 (NCHPh {sym}), 64.7 (NCHPh {asym}), 46.8 (NMe_2 {asym}) 46.0 (NMe_2 {sym}), 45.4 (NMe_2 {asym}), 33.5 (CH_2), 32.9 (CH_2), 32.7 (CH_2), 29.9 (CH_2), 29.3 (CH_2), 28.8 (CH_2).

X-ray Analyses. The X-ray data were collected on a Nonius Kappa CCD (**3**, **10**, and **11**) or a Bruker AXS Smart 1000 CCD diffractometer (**4** and **14**) at low temperature. Crystals of compound **10** were difficult to obtain and weak diffractors. However, despite the poor quality of the data the principle features of the molecular structure (in particular the question of isomeric forms) are well established and are therefore included in this paper. The structures were solved using direct methods with absorption corrections being applied as part of the data reduction scaling procedure. After refinement of the heavy atoms, difference Fourier maps revealed the maxima of residual electron density close to the positions expected for the hydrogen atoms; they were introduced as fixed contributors in the structure factor calculations and treated with a riding model, with isotropic temperature factors but not refined. Full-matrix least-squares refinement was carried out on F^2. A final difference map revealed no significant maxima of residual electron density. Structure solution and refinement were performed using either the SHELX software suite[42,43] or CRYSTALS.[44] The structure of **14** was refined as a racemic twin, with the two components present in a 24:76 ratio. Crystal data and experimental details are provided in Table 2.

Computational Details

The four diastereomeric forms (**I**−**IV**, Figure 5) of [Ti{κ^3-N(2,6-$C_6H_3Me_2$)C(NMe_2)NCH(^{i}Pr)CH_2O}$_2$] (**4**) were calculated using the Gaussian 03 program.[41] ONIOM calculations were performed with [Ti({κ^3-N(Ph)C(NH_2)NCH_2CH_2O}$_2$] being modeled at the QM (B3PW91) level, with the isopropyl groups and the missing methyl groups being calculated at the molecular mechanics level (UFF model). In the QM part of the calculations, all centers were calculated with the 6-31G(d,p) basis set. Geometry optimizations without any symmetry restraints were performed, followed by frequency calculations to ensure the absence of imaginary frequencies. It was found that there were a number of minima around the reported structures, in which the NMe_2 moiety was distorted from trigonal planar to pyramidal. These minima were of almost identical energy to the reported structure but are not considered in this paper

(41) Frisch, M. J.; Trucks, G. W.; Schlegel, H. B.; Scuseria, G. E.; Robb, M. A.; Cheeseman, J. R.; Montgomery, J. A., Jr.; Vreven, T.; Kudin, K. N.; Burant, J. C.; Millam, J. M.; Iyengar, S. S.; Tomasi, J.; Barone, V.; Mennucci, B.; Cossi, M.; Scalmani, G.; Rega, N.; Petersson, G. A.; Nakatsuji, H.; Hada, M.; Ehara, M.; Toyota, K.; Fukuda, R.; Hasegawa, J.; Ishida, M.; Nakajima, T.; Honda, Y.; Kitao, O.; Nakai, H.; Klene, M.; Li, X.; Knox, J. E.; Hratchian, H. P.; Cross, J. B.; Bakken, V.; Adamo, C.; Jaramillo, J.; Gomperts, R.; Stratmann, R. E.; Yazyev, O.; Austin, A. J.; Cammi, R.; Pomelli, C.; Ochterski, J. W.; Ayala, P. Y.; Morokuma, K.; Voth, G. A.; Salvador, P.; Dannenberg, J. J.; Zakrzewski, V. G.; Dapprich, S.; Daniels, A. D.; Strain, M. C.; Farkas, O.; Malick, D. K.; Rabuck, A. D.; Raghavachari, K.; Foresman, J. B.; Ortiz, J. V.; Cui, Q.; Baboul, A. G.; Clifford, S.; Cioslowski, J.; Stefanov, B. B.; Liu, G.; Liashenko, A.; Piskorz, P.; Komaromi, I.; Martin, R. L.; Fox, D. J.; Keith, T.; Al-Laham, M. A.; Peng, C. Y.; Nanayakkara, A.; Challacombe, M.; Gill, P. M. W.; Johnson, B.; Chen, W.; Wong, M. W.; Gonzalez, C.; Pople, J. A. *Gaussian 03*, revision B.03; Gaussian, Inc.: Wallingford, CT, 2004.

(42) Sheldrick, G. M. *SHELXS-86*; University of Göttingen: Göttingen, Germany 1986.

(43) Sheldrick, G. M. *SHELXL-97*; University of Göttingen: Göttingen, Germany 1997.

(44) Watkin, D. J.; Prout, C. K.; Carruthers, J. R.; Betteridge, P. W.; Cooper, R. I. *CRYSTALS*, issue 11; Chemical Crystallography Laboratory: Oxford, U.K., 2001.

since a planar NMe_2 group is the best representative of the experimental data (X-ray structures of **3** and **4**). Modeling the NMe_2 group completely at the DFT level did not alter the computational observations.

Acknowledgment. The authors would like to thank André de Cian for X-ray structure analyses. This work was supported by the Deutsche Forschungsgemeinschaft (SFB 623), the Centre National de la Recherche Scientifique (CNRS), and by the European Union.

Supporting Information Available: Eyring plots and crystallographic information in CIF format. This material is available free of charge via the Internet at http://pubs.acs.org.

IC060809Y